100 Gbps/ C-Band CD Digital Pre-Compensated and Direct-Detection Links with Simple Non-Linear Compensation

100 Gbps/λ C-Band CD Digital Pre-Compensated and Direct-Detection Links With Simple Non-Linear Compensation

Haoyi Wang, Pablo Torres-Ferrera, Giuseppe Rizzelli, Valter Ferrero, *Senior Member, IEEE*, and Roberto Gaudino, *Senior Member, IEEE*

***Abstract*—In the scenario of downstream Passive Optical Networks (PON), we analyze through simulations and experiments a 100 Gbps/λ link using digital signal processing (DSP) over up to 50 km single mode fiber (SMF) in C-band. In particular, we propose chromatic dispersion digital pre-compensation (CD-DPC) and quaternary pulse amplitude modulation (PAM-4) levels optimization at the transmitter side (TX), and simple non-linear compensation (NLC) in combination with adaptive equalization (AEQ) at the receiver side (RX). Regarding NLC, we compare two approaches: a quadratic polynomial function and a square-root-like function respectively. In this paper, we analyze in detail the performances of four proposed options, namely equispaced PAM-4 levels without NLC (baseline case), equispaced PAM-4 levels in combination with NLC, optimized PAM-4 levels without NLC, and optimized PAM-4 levels in combination with NLC. We demonstrate through simulations and experiments that optimized PAM-4 levels can only offer limited enhancement when NLC is applied, and up to 3.3 dB sensitivity gain can be obtained thanks to NLC at RX when setting the optimum parameters, with respect to the baseline case.**

***Index Terms*—100 Gbps, direct-detection, electronic dispersion compensation, non-linear compensation.**

I. Introduction

NEXT-generation Passive Optical Networks (PON) and Data Center Interconnects (DCI), today requiring bit rates well beyond 10 Gbps per wavelength (λ), are under rapid development to support the increasing bandwidth and traffic requirements in the access and short-reach networks. Nowadays, standardization of PON systems with bit rate up to 50 Gbps/λ (50G-PON) is being performed by IEEE and ITU-T [1], [2]. The 50G-PON physical layer will keep the intensity modulation and direct detection (IM-DD) scheme, targeting a reach from 0 to (at least) 20 km over single-mode fiber (SMF) [1]–[4]. The development of 100 Gbps/λ PON (100G-PON) alternatives is a hot research topic, as discussed in previous contributions of our group [5], [6]. Regarding standardization of DCI schemes, very recently the IEEE P802.3cu Task Force completed the IEEE Std 802.3cu-2021, defining 100 Gbps/λ operation over SMF links up to at least 10 km (100GBASE-LR1), using quaternary pulse amplitude modulation (PAM-4) [7]. When PON is operated at very high line rate, such as towards 100 Gbps/λ, the DD link suffers from some limitations, for instance, power fading and low receiver sensitivity. Coherent detection therefore presents a choice. However, up to now, PONs have been sticking to DD and simple Digital Signal Processing (DSP), because DD is better suited to meet the PON low-cost requirements, while systems based on coherent receivers and advanced DSP today still seem too complex, costly, and power consuming [8].

In the high-speed PON and long-reach DCI environments, the main challenges regarding the physical layer at such high bit rate are severe optoelectronic (O/E) bandwidth (BW) limitations, fiber and devices nonlinearity, and inter-symbol interference (ISI) and power fading due to chromatic dispersion (CD) [9]. Our group has performed in previous papers a detailed analysis on the impact and compensation of both O/E BW limitations [10], [11] and CD [5], [6] using DSP. In particular, CD Digital Pre-Compensation (CD-DCP) and adaptive equalization (AEQ) have been proposed to counteract these impairments in the very demanding 100 Gbps/λ C-band scenario preserving DD [5]. In all these previous works, the several non-linear distortion sources (i.e., the modulus square relation between the optical field and detected electrical current for DD, the cosine-like relation between the electrical driving signals and the optical field at the optical IQ-MZ modulator (IQ-MZM) output, and the optical fiber non-linearity), have not been directly compensated. Many non-linear pre- and post-compensations have been proposed in the electronic domain, such as Volterra non-linear equalization (VNLE) or neural-network equalization (NNE) [12]–[15]. However, all these techniques are still very complex as compared with standard DSP implemented in current transceivers. Therefore, in our present contribution, very simple digital non-linear compensation (NLC) techniques, adapted from the proposal of a square-root block in [16], are introduced at the receiver (RX) side to partially compensate for part of the non-linear impairments. In [16], the NLC proposal was mainly analyzed through numerical simulations, only a back-to-back eye diagram after the NLC technique was shown from experimental measurements. In [17], [18], a square-root block (performed in the analog domain by

Manuscript received May 28, 2021; revised August 15, 2021; accepted August 21, 2021. Date of publication August 30, 2021; date of current version September 9, 2021. This work was supported in part by the PhotoNext initiative at Politecnico di Torino. *(Corresponding author: Haoyi Wang.)*

The authors are with the Politecnico di Torino, Department of Electronics and Telecommunications, 10129 Torino, Italy (e-mail: haoyi.wang@polito.it; pablo.torres@polito.it; giuseppe.rizzelli@polito.it; valter.ferrero@polito.it; roberto.gaudino@polito.it).

Digital Object Identifier 10.1109/JPHOT.2021.3107487

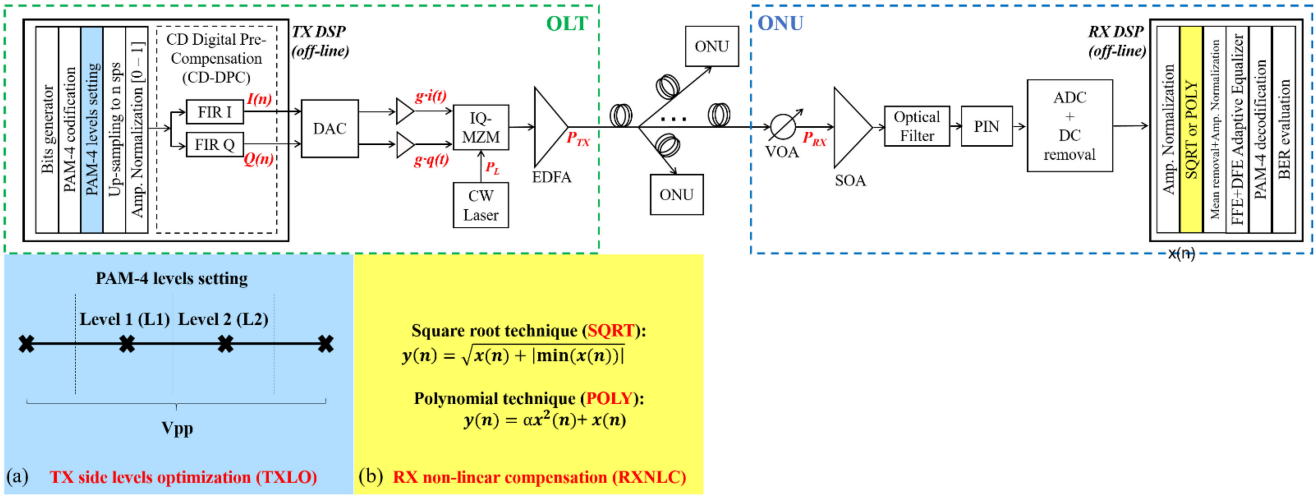

Fig. 1. Top: Experimental and simulation setups. In experiments, the DAC/ADC blocks are inside the AWG/RTO blocks and the total fiber length between EDFA output and VOA input is L=15.80 km, 25.23 km, or 50.46 km. Bottom: (a) TX side levels optimization (TXLO): PAM-4 levels setting was performed at TX side, (b) RX non-linear optimization (RXNLC): POLY and SQRT technologies were applied at RX side. Note: in all cases, enough CD-DCP FIR filters and taps of AEQs were used.

using diodes) has been proposed in Radio-over-Fiber (RoF) system to experimentally show that it helped reduce harmonics at RX side. The square-root module has also been proposed in orthogonal frequency division multiplexing PON (OFDM-PON) system [19], where improvements in terms of optical power budget through simulations have been shown. In this paper, a 100 Gbps/λ C-band DD system using CD-DPC previously reported in [5] is used as a testbed, on top of which we experimentally show up to 3.3 dB gain (and up to 2.4 dB The square-root module has also been proposed in orthogonal frequency division multiplexing PON (OFDM-PON) system [19], where improvements in terms of optical power budget through simulations have been shown. In this paper, a 100 Gbps/λ C-band DD system using CD-DPC previously reported in [5] is used as a testbed, on top of which we experimentally show up to 3.3 dB gain (and up to 2.4 dB gain in simulations) thanks to the proposed simple receiver NLC (RXNLC).

The proposed setup is reported in Fig. 1, where the transmitter (TX) is the same used in our previous paper [5], and the following optical distribution network (ODN) emulates a typical PON scenario. At the RX, we used a Semiconductor Optical Amplifier (SOA) followed by a PIN-photodiode. We indicate as *x(n)* the resulting (normalized) signal after the analog to digital converter (ADC), while *y(n)* is the resulting post-compensated digital signal that inputs the AEQs. The low-complexity digital RXNLC techniques proposed here will be indicated as POLY and SQRT in the following. The first one consists of a quadratic polynomial function applied to the digitized received signal $x(n)$ (normalized to have unit power zero-mean), as shown in Equation (1):

$$y\ (n) = \ x\,(n) + \alpha x^2\,(n) \tag{1}$$

where the coefficient "α" (α-Factor) is a free parameter to be optimized. The second technique consists on a square-root-like function applied to $x(n)$ as defined in Equation (2) and originally proposed in [16]:

$$y\ (n) = \sqrt{x\,(n) + |min\,(x\,(n))|} \tag{2}$$

We will show, both experimentally and by simulations, that these two techniques, despite their simplicity, can improve system performance since, as explained in [16], they partially compensate the asymmetries in the received eye-diagram introduced by the DD square-law detection.

As shown in Fig. 1, we also analyze another simple nonlinear optimization at the TX, consisting on optimizing the PAM-4 levels of the driving signal before applying them to the CD-DPC.

We use as a figure of merit the maximum ODN loss (*Max. ODN loss*) to guarantee a BER target (BER_T) of 10^{-2}. For a fixed transmitted power, the *Max. ODN loss* is directly related to the receiver sensitivity at the BER_T. We analyzed the following four options:

1) PAM-4 equispaced levels (nominal levels) at TX side, without any RX non-linear post-compensation (RXNLC). We termed this scenario as "STD" (from "standard"), using it as the baseline for performance comparison with the three following approaches.
2) PAM-4 optimized levels at TX side without any RXNLC. We termed this scenario as "TXLO" (transmitter levels optimization).
3) PAM-4 equispaced levels at TX side, with only RXNLC. We termed this scenario as "POLY" (if using Eq.1 for RXNLC) or "SQRT" (if using Eq.2 for RXNLC).
4) TXLO in combination with RXNLC. We termed this scenario as "TXLO + POLY" (if using Eq.1 for RXNLC) or "TXLO + SQRT" (if using Eq.2 for RXNLC).

The paper is organized in the following way: the details of simulation and experimental setups are described in Section II. The simulation results comparing the four scenarios in a 16 km fiber link are presented in Section III.A. In Section III.B, we report the experimental results for three fiber lengths: 15.80 km,

25.23 km, and 50.46 km. Finally, we state the main conclusions in Section IV.

II. Experimental and Simulation Setup

A. Simulation Setup

The simulation setup is schematically illustrated in Fig. 1 and described in detail in [5]. We set all the simulation parameters to emulate our experimental system. At the TX side, a PRBS-15 pseudorandom binary sequence (repeated six times, for a total of about $2{\cdot}10^5$ bits, sufficient to have a very reliable BER counting estimation for $BER_T = 10^{-2}$) is generated at bit rate $R_b = 100$ Gbps, and then coded to generate a PAM-4 sequence. We then use the IQ-DD approach that our group proposed in [5], trying anyway to optimize PAM-4 levels when indicated. In fact, due to system non-linear distortions, non-equispaced PAM-4 levels could result in better performance than using the nominal PAM-4 equispaced ones (such as $\{-3\ -1\ +1\ +3\}$). Therefore, to perform a TX side levels optimization (TXLO), a block to set the desired PAM-4 levels is added. As shown in Fig. 1(a), the two PAM-4 outer levels are fixed while the two intermediate levels Level 1 (L1) and Level 2 (L2) are varied. By then varying the peak-to-peak voltage (V_{pp}) of the driving signal at the input of a dual-arm IQ-MZM, the outer levels can also be optimized. In our simulation, an IQ-MZM optical transmitter is assumed, operating in C-band, followed by an ideal optical amplifier to set the transmitted power P_{TX} equal to 11 dBm. We set the IQ-MZM static insertion loss equal to 7 dB plus a dynamic modulation loss that depends on the characteristics of the driving signals. Then, the optical modulated signal is propagated over a conventional ITU-T G.652 single mode fiber (SMF) with length $L = 16$ km, used in C-band at reference wavelength $\lambda = 1550$ nm (attenuation 0.22 dB/km, chromatic dispersion $D = 17$ ps/(nm•km), fiber non-linear coefficient of $26{\cdot}10^{-21}$ m^2/W, and effective area of 80 μm^2 [20]). Kerr nonlinearities are introduced using the conventional non-linear Schrodinger equation (NLSE) solved numerically by the split-step Fourier method. The received optical power (ROP) is measured after a variable optical attenuator (VOA). At the RX side, an optical filter with 75 GHz BW is placed between the SOA (with gain 11dB and noise figure 7.5 dB) and the photodiode PIN. Second order low-pass super Gaussian filters (SGF) were used to emulate the O/E BW limitations both at TX and RX side. To emulate a 25G-class system a TX and RX -3dB BW $f_{3dB} = 20$ GHz and 35 GHz is set, respectively. The receiver parameters are: photodiode responsivity $R = 0.7$ A/W, and TIA input referred noise density $IRND = 12$ pA/sqrt(Hz). Digital-to-analog (DAC) and analog-to-digital converters (ADC) with a 6 bits resolution for quantization are used to emulate the arbitrary waveform generator (AWG) and real-time oscilloscope (RTO) used in the experiment, respectively. The digital signal *x(n)* is obtained after DC removal and amplitude normalization block that sets the signal to have unit power (i.e., variance). At the RX DSP, the received digital signal is post-processed by using the RXNLC, i.e., POLY and SQRT, as shown in Fig. 1(b) with two simple non-linear functions, to partially compensate the non-linearity, as described in the previous Section. After RXNLC, the mean of signal *y(n)* is

removed, and its amplitude is normalized again. A feed forward equalization (FFE) stage with 120 taps, working at 2 samples per symbol (SpS), followed by a decision feedback equalization (DFE) stage with 5 taps, working at 1 SpS, are applied to *y(n)* to compensate for remaining linear impairments. A low-density parity check (LDPC) code FEC scheme with a pre-FEC BER target of 10^{-2} has been defined in the 25G-PON standard [21]. The same pre-FEC BER target is under consideration for the development of 50G-PON [1]. Therefore, as the performance metric, we used the required ROP (RROP) at $BER_T = 10^{-2}$, and the resulting ODN loss, defined as the difference between the transmitted optical power P_{TX} and the received one (i.e., *ODN loss*, dB $= P_{TX}$ – ROP in dBm), and *Max. ODN loss*, dB $= P_{TX}$ – RROP in dBm. As described in ITU-T recommendation [22], the ODN loss is one of the most important parameters to define the overall system performance.

B. Experimental Setup

The experimental setup, described in detail in [5], is also shown in Fig. 1. DAC and ADC are inside the 92 GS/s AWG and 200 GS/s RTO, respectively. At the off-line TX DSP, a PAM-4 signal is generated and processed. The signal is then up sampled to 1.84 SpS to match the sampling frequency of the AWG. Then a frequency pre-emphasis (PE) block is applied to partially pre-compensate transmitter electronic bandwidth limitations. The PE is implemented by using a one-pole inverse low-pass filter [5] with a 12 GHz cut-off frequency, value obtained after optimization during the experimental campaign for the different configurations analyzed here. The resulting signal is fed to the CD-DPC block [5], [6]. The laser central wavelength is 1549 nm. After the 25G-class IQ-MZM, the optical modulated signal is amplified by an EDFA (used to boost the transmitted average power). The optical signal is propagated over a conventional ITU-T G.652 SMF (15.80 km, a distance basically corresponding to the one used in our simulations, 25.23km or 50.46 km). Then it is sent to a VOA (to change the ODN loss), a SOA, a 10-nm optical filter, a 50G-class photodiode PIN+TIA and the RTO. At off-line RX DSP, the received signal is post-processed at 2 SpS, and followed by RXNLC and AEQs, using the same blocks described in the simulation setup.

III. Results

A. Simulation Results

In order to set up and better understand the following experiments, we performed a set of simulations. The simulation results are obtained setting a fiber length $L = 16$ km and transmitted optical power $P_{TX} = 11$dBm. The peak-to-peak swing V_{pp} of driving signal is optimized for every pre-compensated length L_C (set in CD-DCP algorithm) [5], every ODN loss and every scenario. Fig. 2 shows the contour plot of Max. ODN loss metric (in dB) vs. PAM-4 level optimization, for three different cases: TXLO in Fig. 2(a), TXLO+POLY in Fig. 2(b), and TXLO+SQRT in Fig. 2(c). All the simulation results in Fig. 2

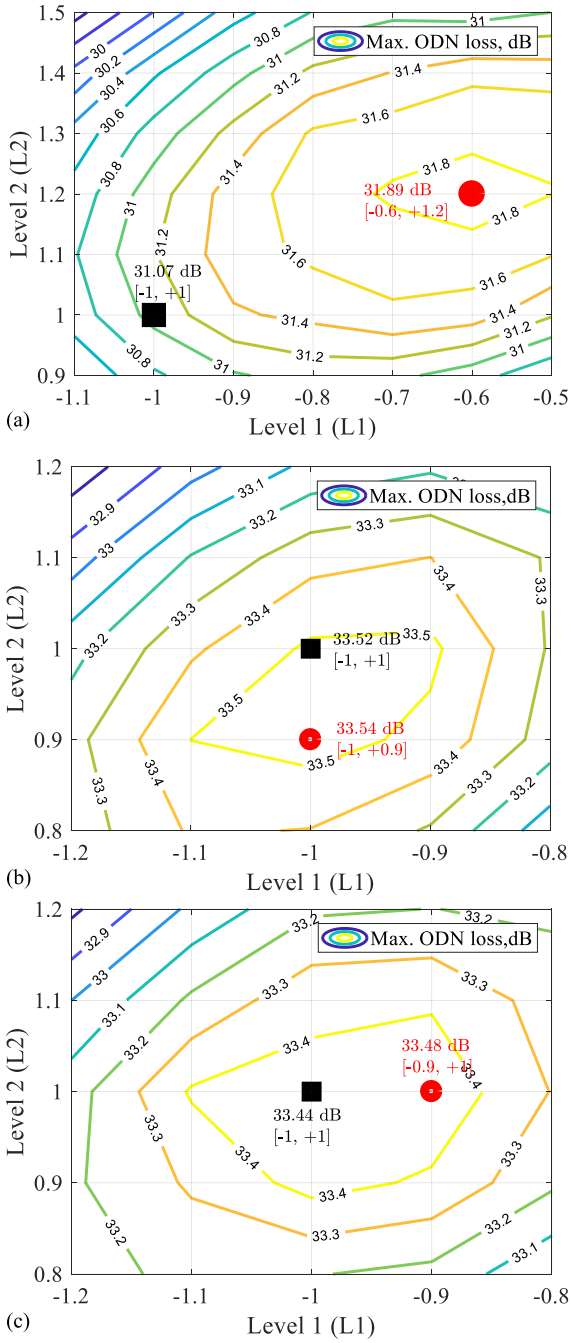

Fig. 2. Maximum ODN loss as a function of two internal levels of PAM-4 signal level 1 (L1) and level 2 (L2), for $L = 16$ km, $Lc = 15$ km and $P_{TX} = 11$ dBm, with the optimum V_{pp} of driving signal: (a) without any RXNLC, (b) with POLY, (c) with SQRT. Red dot: with TXLO (i.e., optimum internal levels L1 and L2 for PAM-4 signal). Black rectangle: without TXLO (i.e., nominal internal levels L1 and L2 for PAM-4 signal [-1, +1]).

are obtained with $L_C = 15$ km, which is the optimum value of L_C when $L = 16$ km (details in [5]). For the POLY case, we used $\alpha\text{-}Factor = -0.16$ (the optimum α-Factor for this case, see later for a detailed discussion of this parameter). The red dot shows the Max. ODN loss at the optimum L1-L2 pair (i.e., when the TXLO was applied), while black rectangle shows the Max. ODN loss at the nominal L1-L2 pair of PAM-4 signal (i.e., [-1, +1]).

For the three analyzed cases (TXLO, TXLO+POLY and TXLO+SQRT), the optimum L1-L2 pair are [-0.6, +1.2], [-1, +0.9] and [-0.9, +1], and the Max. ODN loss are 31.89 dB, 33.54 dB and 33.48 dB. These results, that will be confirmed by experiments in the next sections, shows the main results of our paper, in particular:

1) Transmitter level optimization (TXLO) without nonlinear compensation at the receiver gives about 0.8 dB advantage in Max. ODN loss.
2) Better performance can anyway be gained with the simple nonlinear compensation at the receiver (either SQRT or POLY). In this case, the difference between STD (TX nominal levels) or TXLO (TX optimized levels) become negligible, and thus TXLO can be avoided. The difference between SQRT or POLY approaches is also negligible.
3) Overall, the difference between no optimization at all (giving about 31.1 dB in Fig. 2(a) and any of the receiver nonlinear techniques (giving about 33.5 dB) is a significant 2.4 dB, which is the main achievement of our proposal.

A heuristic explanation of these results is in the non-linearity we mentioned before, which originates from the modulus square relation between the optical field and detected electrical current for DD, the cosine-like relation between driving signal and optical field at the output of the optical IQ-MZ modulator and the fiber non-linearity. It can be partially compensated by the RXNLC (POLY or SQRT). As for RXNLC SQRT, Eq.1 used for POLY is essentially the Taylor expansion of Eq.2 used for SQRT. RXNLC POLY will converge to SQRT at its optimum α-Factor. Considering the α-Factor in RXNLC POLY, changing α-Factor is equivalent to changing two internal levels L1 and L2 of PAM-4 signal, which is the same as TXLO. Therefore, we can neglect the TXLO when the RXNLC is adopted. Moreover, the complexity of RXNLC is much lower than that of the TXLO, because the optimization that is done at the TX requires in practice a feedback from the receiver (i.e., a metric evaluated at the receiver, such as BER or eye opening), which is much more difficult to be implemented in a real transceiver.

We also analyze the impact of varying the α-Factor in the POLY approach. Fig. 3 shows the Max. ODN loss in dB obtained at the optimum $Lc = 15$ km (note that the Max. ODN loss is independent of the α-Factor for STD, TXLO, SQRT and TXLO+SQRT, so that they appear in the graphs vs. α as horizontal lines). Solid and dashed curves are the two cases without and with TXLO respectively. Compared with the baseline STD (solid black curve), a gain of about 0.8 dB in terms of Max. ODN loss is obtained by applying TXLO, and a significant gain of about 2.5 dB can be reached by applying RXNLC. Consistently with Fig. 2, the TXLO can only improve the performance when POLY or SQRT is not applied (as shown in the black solid and dashed curves in the figure), because RXNLC is equivalent to TXLO in terms of changing the two internal levels L1 and L2 of PAM-4 signal. The Max. ODN loss of POLY changes as the α-Factor changes. According to the equation of RXNLC POLY in Eq.1, POLY is equivalent to STD when $\alpha = 0$. And the optimum $Max.\ ODN\ loss = 33.54$ dB is obtained when the α-Factor is -0.16, which is very close to that of SQRT, i.e., 33.48

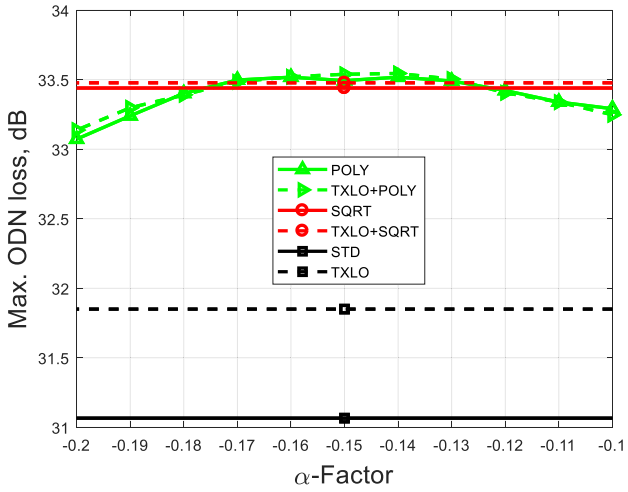

Fig. 3. Maximum ODN loss as a function of α-Factor (for POLY and TXLO+POLY), for $L = 16$ km, $Lc = 15$ km and $P_{TX} = 11$ dBm, with the optimum V_{pp} of driving signal. Solid: without TXLO. Dashed: with TXLO.

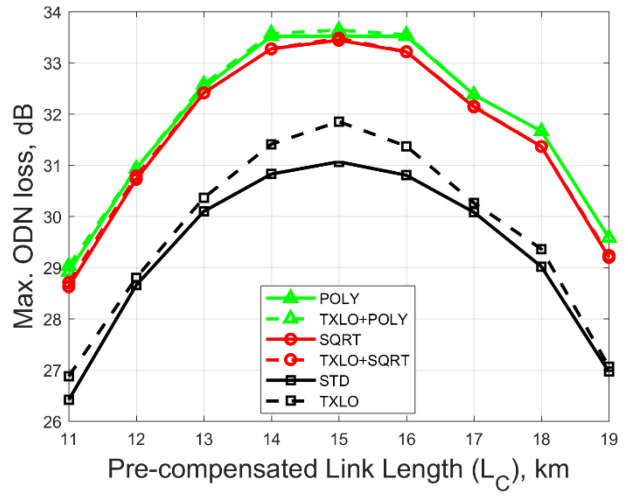

Fig. 4. Maximum ODN loss as a function of Lc, for $L = 16$ km and $P_{TX} = 11$ dBm, with the optimum V_{pp} of driving signal. Solid: without TXLO, dashed: with TXLO.

dB. This experimentally verified that POLY has a very similar performance to SQRT at the optimum α-Factor.

We continue by analyzing the performance comparison among different scenarios not only at the optimum L_C but over a wide L_C range, i.e., from 11 to 19 km. The details of the CD-DPC are reported in [5]. Here we just briefly remind that L is the fiber physical length, while L_C is the length assumed for designing the taps of the FIR filter used for CD pre-compensation at the transmitter, which thus assume to compensate an accumulated dispersion $D \cdot L_C$. Fig. 4 presents the Max. ODN loss in dB as a function of L_C. Solid and dashed curves show the performance without and with TXLO respectively. The optimum L_C is 15 km for all the scenarios. It is interesting to note that the optimum L_C is slightly shorter than L, because the dispersion can be partially compensated by the self-phase modulation induced by Kerr effect [5]. As observed before in Fig. 2 and Fig. 3, comparing STD and TXLO, the gains in terms of Max. ODN

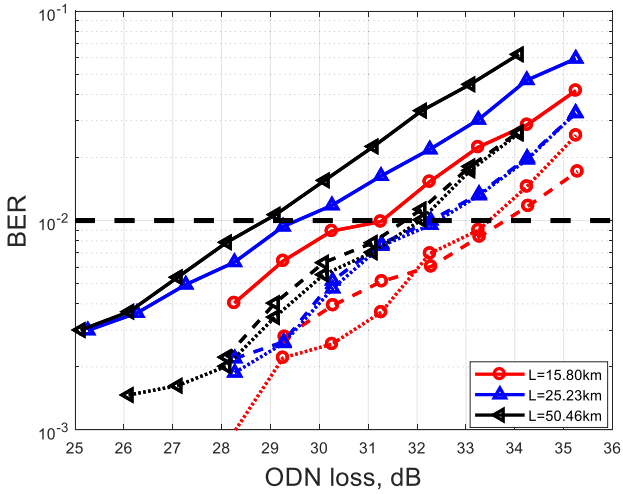

Fig. 5. BER as a function of ODN loss with different fiber length L and $P_{TX} = 11$ dBm at optimum L_C (14.80 km, 24.23 km, and 48.46 km for $L = 15.80$ km, 25.23 km, and 50.46 km respectively), with the optimum V_{pp} of driving signal and without any TXLO. Solid: STD, dashed: POLY, and dotted: SQRT.

loss are about 0.2-0.8 dB for all L_C values. On the contrary, when comparing POLY/SQRT and TXLO+POLY/SQRT, the gains are very limited to less than 0.1dB. The improvement produced by TXLO disappeared because POLY/SQRT is equivalent to TXLO with regard to finding the optimum L1-L2 pair of PAM-4 signal. However, compared to the baseline scenario STD (solid black curve in Fig. 4), gains of 2-2.7 dB were obtained by applying TXLO+POLY/SQRT for all L_C values. The performance of applying POLY/SQRT alone is better than that of applying TXLO alone (gains of about 0.2-0.8 dB as mentioned before). As an intuitive explanation of why a simple square-root law can improve performance, we remind that our system (similar to the one in [16]) is field-modulated at the transmitter and uses optical pre-amplifier at the receiver. Thus, the system can be classified as a linear additive Gaussian noise channel on the field. Anyway, the photodiode acts as a square law detector, thus destroying this linearity on the signal at its output. The SQRT (or similarly the POLY) correction partially restore the linearity on the signal and the noise, which (to a first approximation) becomes again additive Gaussian. The results are compatible with previous results at the optimum $L_C = 15$ km, and a gain of round 2-2.7 dB appears for all L_C values.

B. Experimental Results

In this Section, we present our main experimental results, using different fiber lengths L and transmitted optical power $P_{TX} = 11$dBm.

Fig. 5 shows experimental measured BER vs. ODN loss for three SMF fiber lengths without any TXLO to compare with previous simulations and our previous work [5]. The significant enhancement of up to 2.7 dB in terms of ODN loss by applying POLY/SQRT (anticipated by the simulations) is also experimentally verified for all the three cases. Note that the V_{pp} of driving signal is optimized for every ODN loss and every scenario. The performance of POLY/SQRT are very similar

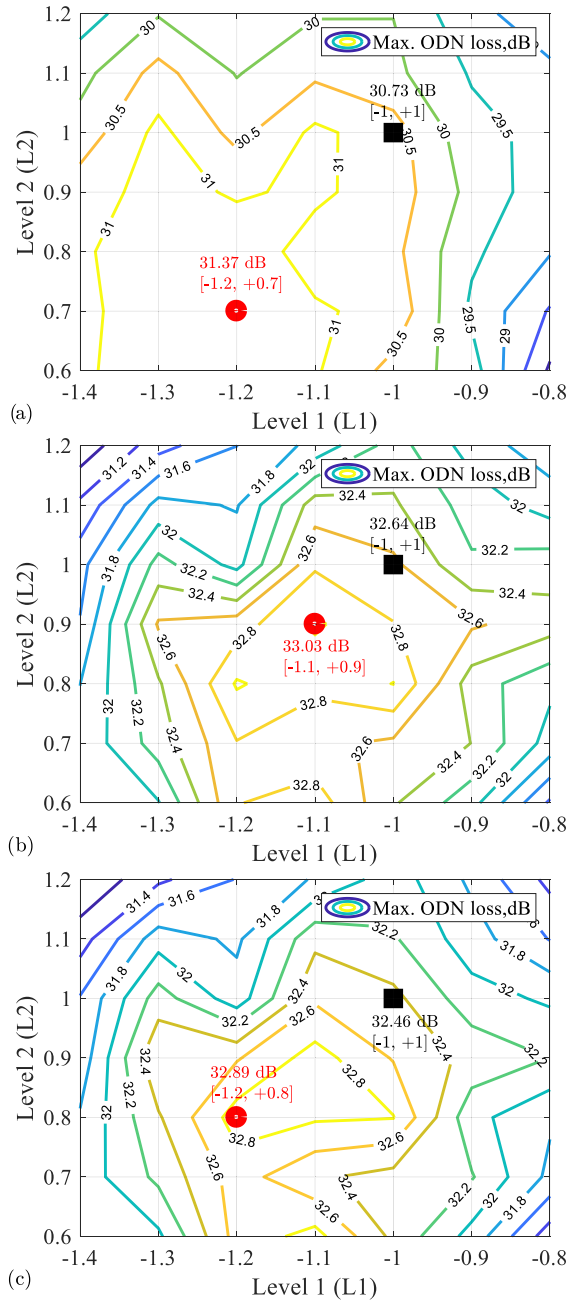

Fig. 6. Experimental Maximum ODN loss as a function of two internal levels of PAM-4 signal Level 1 (L1) and Level 2 (L2), for $L = 15.80$ km, $Lc = 14.80$ km and $P_{TX} = 11$ dBm, with the optimum V_{pp} of driving signal: (a) without any RXNLC, (b) With POLY, (c) With SQRT. Red dot: with TXLO (i.e., optimum internal levels L1 and L2 for PAM-4 signal). Black rectangle: without TXLO (i.e., nominal internal levels L1 and L2 for PAM-4 signal [-1, +1]).

which is consistent with previous simulation results. Three SMF fibers, each with different length, were analyzed. The 25.23 km and 50.46 km ones are studied for comparison to previously reported experimental results. In [5], experimental results using the same experimental setup were reported, using 25.23 km and 50.46 km fibers and a transmitted power of 11 dBm. As shown in Fig. 6(b) of [5], a Max. ODN loss of 29 dB and 28.5 dB is achieved for 25.23 and 50.46 km, respectively, under these conditions without any RXNLC technique but using optimized

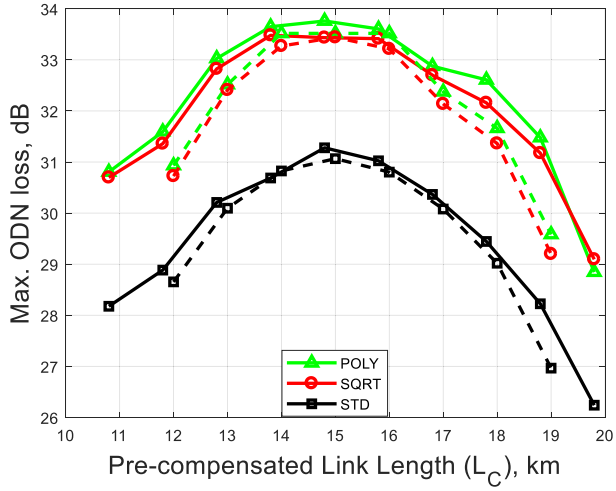

Fig. 7. Maximum ODN loss as a function of Lc, with the optimum V_{pp} of driving signal. Solid: experiments with $L = 15.8$ km and $P_{TX} = 11$ dBm. Dashed: simulations with $L = 16.0$ km and $P_{TX} = 11$ dBm (dashed curves extracted from Fig. 4).

PAM-4 levels. As shown in Fig. 5, the Max. ODN loss of about 29 dB with 50.46 km fiber is obtained at BER_T, which is slightly better and showing a good match with our previous publication. As experimental results shown in Fig. 6(a) of [5], with a 25 km fiber and a transmitted power of 11 dBm, the Max. ODN loss without any RXNLC was about 29 dB at the optimum L_C. As shown in Fig. 5, we obtained a better Max. ODN loss of about 29.5 dB at BER_T. In the rest of the paper, we will focus on $L = 15.8$ km with $P_{TX} = 11$ dBm case (the case studied on purpose also in the previous simulation Section), to target a typical PON fiber length.

To experimentally verify the limited enhancement of the TXLO technique mentioned in the previous simulation results section (when RXNLC is applied), the contour plots of the measured Max. ODN loss as a function of two internal levels L1 and L2 are shown in Fig. 6. We present the experimental results at the optimum $L_C = 14.8$ km. The red dot shows the Max. ODN loss at its optimum L1-L2 pair (i.e., when the TXLO was applied), and the black rectangle shows the Max. ODN loss at the nominal L1-L2 pair of PAM-4 signal (i.e., [-1, +1]). The optimum L1-L2 pair are [-0.6, +1.2], [-1, +0.9] and [-0.9, +1], and the Max. ODN loss are 31.37 dB, 33.03 dB and 32.89 dB for TXLO, TXLO+POLY, and TXLO+SQRT respectively. The Max. ODN loss at the nominal L1-L2 pair are 30.73 dB, 32.64 dB and 32.46 dB for TXLO, TXLO+POLY, and TXLO+SQRT respectively. From Fig. 6(b) and Fig. 6(c) for cases with RXNLC (i.e., with POLY or SQRT), the differences of the Max. ODN loss between the optimum L1-L2 pair (with TXLO) and the nominal L1-L2 pair (without TXLO) are only less than 0.5 dB, confirming the simulation results of Fig. 2, where the comparison between optimum and nominal levels, was less than 0.1 dB in terms of ODN loss. The experimental environment is more realistic and complex and resulting in a little higher difference. Due to this limited improvement of the TXLO technique, we avoided TXLO in the rest of our experiments, so we use only PAM-4 nominal levels.

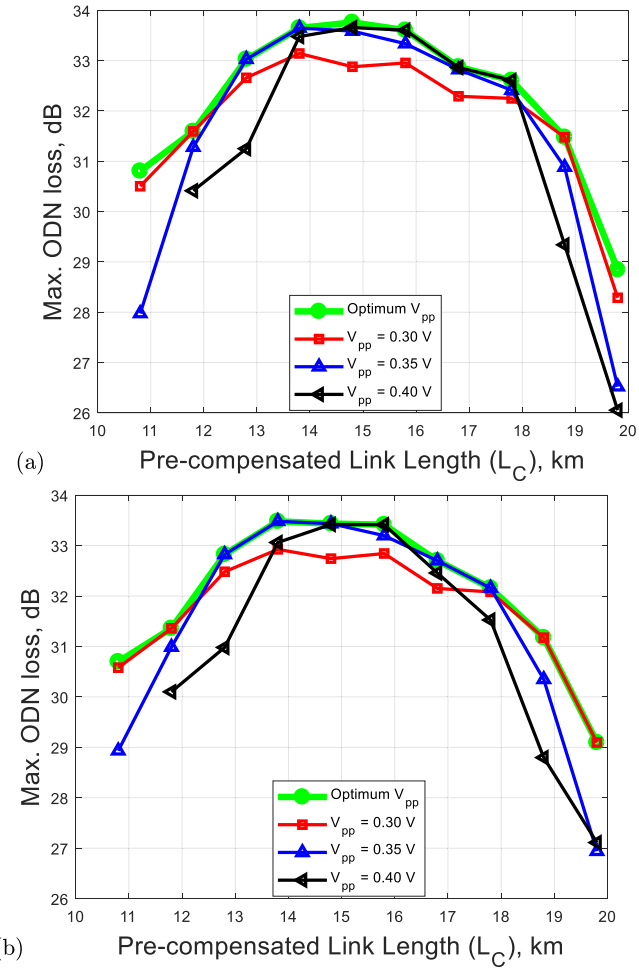

Fig. 8. Maximum ODN loss as a function of Lc with $L = 15.8$ km and $P_{TX} = 11$ dBm, for different V_{pp} values (sub-optimum performance) and optimum V_{pp} (optimum performance, green curves with optimum V_{pp} are extracted from Fig. 7).(a) with POLY and (b) with SQRT.

We continue by analyzing the experimental performances not only at the optimum L_C but over a wide L_C range from 10.8 km to 19.8 km and comparing experimental with simulation results as well. Fig. 7 shows Max. ODN loss as a function of L_C for the different cases. Note that the V_{pp} of driving signal is optimized for every pre-compensated length L_C, every ODN loss and every technique. Experimental results are shown in solid curves, and dashed curves represent the previous simulation results. The optimum L_C is 14.8 km, which is about 1 km shorter than L and is compatible with previous simulation results. Two techniques POLY and SQRT are presenting a similar performance over the whole L_C range. The experimental results are remarkably consistent with the simulation ones, which experimentally confirmed the simulation results we mentioned in Section 3.1. Compared to the baseline scenario STD (solid black curve), gains from 2.1 dB and up to 3.3 dB were obtained by applying RXNLC (POLY or SQRT) for all L_C values (gains from 2 dB and up to 2.7 dB were obtained in previous simulations). The non-linear distortions over DD link can be partially compensated by a simple RXNLC and results in a significant enhancement in terms of Max. ODN loss over L_C range.

In Fig. 8 we further investigate on the optimization of V_{pp} driving signal that ensures a better performance, reporting results for three different V_{pp}, while green curves show the performances with an optimized V_{pp} for every technique, ODN loss and Lc value (note that in all the previous results shown in this Section, the V_{pp} was optimized). For the scenarios with the optimized V_{pp}, our techniques work for a wider range of Lc (i.e., from 10.8 km to 19.8 km) with the Max. ODN loss ≥ 29 dB. For the ones with a single fixed V_{pp}, the tolerance ranges of L_C are narrower as the V_{pp} increases. On the contrary, the Max. ODN loss at L_C which around the optimum L_C increases as the V_{pp} increases. Especially with the lowest $V_{pp} = 0.3$ V, the penalty with respect to the case with the optimum V_{pp} is about 1 dB. It is the trade-off between the system complexity and performance. With the best fixed V_{pp} (0.35 V in this case), a performance close to the optimum one can be guaranteed for the most of L_C ranges (except for the extreme values of the L_C range, i.e., L_C from 11.8 km to 18.8 km). For the Lc within the range 11.8–18.8 km, the optimization of V_{pp} can be avoided to reduce the complexity.

IV. Conclusion

Elaborating on the pre-distortion proposal presented in [5], we further improved its performances introducing some simple optimization in the TX or RX DSP. We show that on a 100 Gbps C-band PON environment using DD, a considerable improvement in terms of Max. ODN loss is achieved by combining CD-DCP at TX DSP and AEQs and RXNLC at RX DSP.

We also propose a TXLO by varying the two intermediate levels L1 and L2 of PAM-4 signal, and we demonstrate through simulations and experiments that the improvement was very limited when RXNLC was already applied. Therefore, TXLO can be avoided. We verified through both simulations and experiments that the performances of POLY and SQRT are very similar. The simple POLY/SQRT can present a good choice because of the considerable gain (about 2 dB) in terms of Max. ODN loss over a wide L_C range and preserving a low complexity added at only RX side. For $L = 15.8$ km and $P_{TX} = 11$ dBm, optimization at TX side (both TXLO and optimization of V_{pp}) can be avoid when Lc within the range 11.8–18.8 km.

As a final comment for application to PON, the proposed system can enable again the use of the C-band even at extremely high bit rates toward 100Gbit/s sticking with DD receiver, while all recent standards had to move to the O-Band. Our proposal works well for a given fiber length L, with a tolerance of ± 2 km (as shown in Figs. 7 and 8) and it is thus perfectly tailored for P2P over PON on a dedicated wavelength. For normal TDMA downstream PON applications, in which the length can vary from 0 to 20 km, further improvements in the TX DSP algorithm are needed, as discussed in the Conclusion of our previous paper [5].

Acknowledgment

The author thank the support of the PhotoNext initiative at Politecnico di Torino. This work has been carried out in the framework of a research contract with Telecom Italia Lab (the TIM company research laboratory).

REFERENCES

[1] D. Zhang, D. Liu, X. Wu, and D. Nesset, "Progress of ITU-T higher speed passive optical network (50G-PON) standardization," *EEE/OSA J. Opt. Commun. Netw.*, vol. 12, no. 10, pp. D99–D108, Oct. 2020.

[2] E. Harstead *et al.*, "Technology roadmap for time-division multiplexed passive optical (TDM PONs), " *J. Lightw. Technol.*, vol. 37, no. 2, pp. 657–664, 2019.

[3] ITU-T G.9804.1 "Higher speed PON requirements," Sep. 2011, [Online]. Available: https://www.itu.int/itu-t/recommendations/rec.aspx?rec=14024

[4] H. Wang, P. Torres-Ferrera, V. Ferrero, A. Pagano, R. Mercinelli, and R. Gaudino, "Current trends towards PON systems at 50+ Gbps," in *Proc. Italian Conf. Opt. Photon.*, Parma, Italy, 2020, pp. 1–4.

[5] P. Torres-Ferrera, G. Rizzelli, V. Ferrero, and R. Gaudino, "100+ Gbps/λ 50 km C-band downstream PON using CD digital pre-compensation and direct-detection ONU receiver," *J. Lightw. Technol.*, vol. 38, no. 24, pp. 6807–6816, Dec. 2020.

[6] P. Torres-Ferrera, H. Wang, V. Ferrero, and R. Gaudino, "100 Gbps/λ PON downstream O- and C-band alternatives using direct-detection and linear-impairment equalization," *IEEE/OSA J. Opt. Commun. Netw.*, vol. 13, no. 2, pp. A111–A123, Feb. 2021.

[7] IEEE P802.3cu 100 Gb/s and 400 Gb/s over SMF at 100 Gb/s per wavelength task force, Accessed: Mar. 3, 2021, [Online]. Available: https://www.ieee802.org/3/cu/

[8] V. Houtsma, A. Mahadevan, N. Kaneda, and D. van Veen, "Transceiver technologies for passive optical networks: Past, present, and future," *IEEE/OSA J. Opt. Commun. Netw.*, vol. 13, no. 1, pp. A44-A55, Jan. 2021.

[9] Z. Zhang *et al.*, "Optical- and electrical-domain compensation techniques for next-generation passive optical networks," *IEEE Commun. Mag.*, vol. 57, no. 4, pp. 144–150, Apr. 2019.

[10] P. Torres-Ferrera, V. Ferrero, M. Valvo, and R. Gaudino, "Impact of the overall electrical filter shaping in next-generation 25 and 50 Gb/s PONs," *IEEE/OSA J. Opt. Commun. Netw.*, vol. 10, no. 5, pp. 493–505, May 2018.

[11] P. Torres-Ferrera, H. Wang, V. Ferrero, M. Valvo, and R. Gaudino, "Optimization of band-limited DSP-aided 25 and 50 Gb/s PON using 10G-class DML and APD," *J. Lightw. Technol.*, vol. 38, no. 3, pp. 608–618, Feb. 2020.

[12] J. Zhang *et al.*, "Decision-feedback frequency-domain volterra nonlinear equalizer for IM/DD OFDM long-reach PON," *J. Lightw. Technol.*, vol. 37, no. 13, pp. 3333–3342, Jul. 2019.

[13] S. Lu, C. Wei, C. Chuang, Y. Chen, and J. Chen, "81.7% complexity reduction of volterra nonlinear equalizer by adopting L1 regularization penalty in an OFDM long-reach PON," in *Proc. Eur. Conf. Opt. Commun.*, 2017, pp. 1–3.

[14] L. Yi, T. Liao, L. Huang, L. Xue, P. Li, and W. Hu, "Machine learning for 100 Gb/s/λ passive optical network," *J. Lightw. Technol.*, vol. 37, no. 6, pp. 1621–1630, Mar. 2019.

[15] V. Houtsma, E. Chou, and D. van Veen, "92 and 50 Gbps TDM-PON using neural network enabled receiver equalization specialized for PON," in *Proc. Opt. Fiber Commun. Conf. Exhib.*, 2019, pp. 1–3.

[16] J. Prat, A. Napoli, J. M. Gene, M. Omella, P. Poggiolini, and V. Curri, "Square root strategy: A novel method to linearize an optical communication system with electronic equalizers," in *Proc. 31st Eur. Conf. Opt. Commun.*, 2005, pp. 713–714.

[17] J. Prat, M. C. Santos, and M. Omella, "Square root module to combat dispersion-induced nonlinear distortion in radio-over-fiber systems," *IEEE Photon. Technol. Lett.*, vol. 18, no. 18, pp. 1928–1930, Sept. 2006.

[18] J. Prat *et al.*, "Electronic equalization of photodetection by means of an SQRT module," in *Proc. 9th Int. Conf. Transparent Opt. Netw.*, 2007, pp. 251–256.

[19] Pravindra Kumar and Anand Srivastava, "Optical power budget enhancement in next-generation DDO-OFDM-based optical access networks using square root module," *Photonic Netw. Commun.*, vol. 31, no. 1, pp. 48–55, 2015.

[20] *ITU-T Recommendation ITU-T G.652 (11/2016), SERIES G: TRANSMISSION SYSTEMS AND MEDIA, DIGITAL SYSTEMS AND NETWORKS*, Transmission media and optical systems characteristics—Optical fibre cables, "Characteristics of a single-mode optical fibre and cable."

[21] *IEEE. IEEE Standard for Ethernet Amendment 9: Physical Layer Specifications and Management Parameters for 25 Gb/s and 50 Gb/s Passive Optical Networks*. IEEE Std 802.3ca-2020.

[22] *ITU-T Recommendation ITU-T G.984.2 (08/2019), SERIES G: TRANSMISSION SYSTEMS AND MEDIA, DIGITAL SYSTEMS AND NETWORKS*. Digital sections and digital line system—Optical line systems for local and access networks, "Gigabit-capable passive optical networks (GPON): Physical media dependent (PMD) layer specification."